Review of Solar Thermoelectric Energy Conversion and
Analysis of a Two Cover Flat-Plate Solar Collector

by

Atiya Hasan

Submitted to the Department of Mechanical Engineering in
Partial Fulfillment of the Requirements for the Degree of

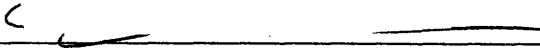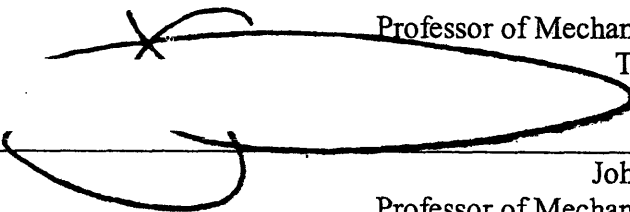Bachelor of Science in Engineering

at the

Massachusetts Institute of Technology

February 2007

The author hereby grants to MIT permission to reproduce and to distribute
publicly paper and electronic copies of this thesis document in whole or in
part in any medium now known or hereafter created.

Signature of Author _____

Department of Mechanical Engineering

January 30, 2007

Certified by _____

Gang Chen

Professor of Mechanical Engineering

Thesis Supervisor

Accepted by _____

John H. Lienhard V

Professor of Mechanical Engineering

Undergraduate Officer, Department of Mechanical Engineering
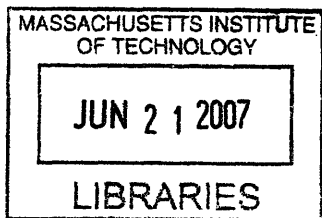
1

Review of Solar Thermoelectric Energy Conversion and
Analysis of a Two Cover Flat-Plate Solar Collector

by

Atiya Hasan

Submitted to the Department of Mechanical Engineering
on January 30, 2007 in Partial Fulfillment of the Requirements for the
Degree of Bachelor of Science in Mechanical Engineering

ABSTRACT

The process of solar thermoelectric energy conversion was explored through a review of
thermoelectric energy generation and solar collectors. Existing forms of flat plate
collectors and solar concentrators were surveyed.

A thermal analysis of a common two-cover flat plate solar collector was then performed.
The model focused specifically on radiation absorption through the cover system and
radiation and convection losses from the absorption plate to determine the parameters that
most significantly affect the efficiency of the collector and the overall efficiency of the
solar thermoelectric generator. In this case, collector efficiency was measured by the
ratio of useable energy to incident solar energy. Overall generator efficiency was
measured by power generated per unit area of the collector.

It was found that of several parameters, the collector area had the most significant
influence on collector efficiency. For the overall efficiency of the generator, the most
significant parameter was the ratio of the collector area to the cross-sectional area of the
thermoelectric elements (TE). The efficiency of the generator maximized at a ratio of
250:1, with a magnitude of 5.76 W/m^2. The analysis exposes some weaknesses of the flat
plate collector to show where future designs should focus for improvement.

Thesis Supervisor: Gang Chen

Title: Professor of Mechanical Engineering

Table of Contents

Chapter 1: Introduction

1.1   Solar Thermoelectric Energy Conversion

Solar thermoelectric energy generation is the process of turning solar radiation

into useable electric energy through thermoelectric energy conversion. The process takes

advantage of the Seebeck effect, in which a circuit with a maintained temperature

difference across a conductor induces a current. To force the temperature difference, a

constant source of thermal energy is needed. One obvious resource is the sun, which has

practically no limit when it comes to its potential as a supplier of energy for small scale

power generation. Solar radiation is constant and predictable, which makes it a natural

choice to collect and use in energy conversion.
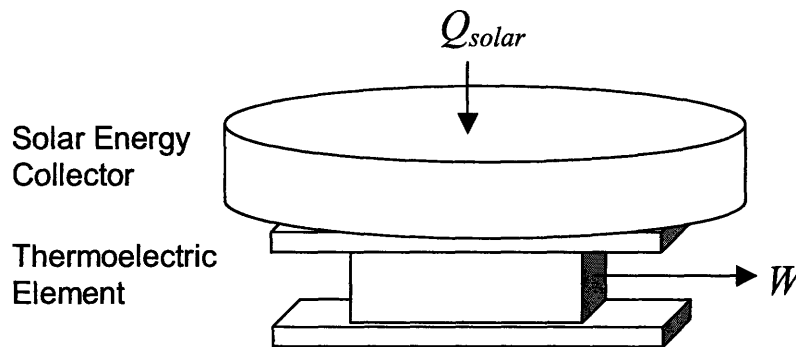
Figure 1.1: A representation of a solar thermoelectric energy conversion
device with its two components, the solar energy collector and
the thermoelectric element.

As shown in figure 1.1, the devices used in solar thermoelectric energy generation

consist of two components. The first is the collector, which traps solar radiation in the

form of thermal energy. The second component is the thermoelectric element (TE),

which uses the trapped thermal energy to heat its hot junction and generate a current.

The design of the thermoelectric component has been standardized, but configurations of solar collectors vary widely. Solar energy collectors, normally used for simple air or water heaters, are geometrically designed to maximize radiation absorption and thermally designed to transfer the energy to the flowing target fluid. Their design needs some adjustment when used for thermoelectric purposes.

1.2 Uses and Advantages

The advantages of a solar thermoelectric conversion system are many. The first and most obvious is the harnessing of solar energy, which until today is realized to only a very small fraction of its potential. Scientists are constantly seeking out efficient, clean, and economical fuel sources that the world desperately needs. Any energy generation system that fulfills any of the three criteria merits deeper exploration. Solar energy has the potential to meet all three.

In the specific case of thermoelectric energy conversion, one major advantage is the simplicity of the device. As shown in figure 1.2, a thermoelectric energy generator with a flat plate solar collector is essentially several sheets of glass and metal attached to a simple circuit of semiconductors. There are no moving parts and no chemical reactions occurring in the system, which means that there are few maintenance requirements due to wearing out or corrosion. For these reasons, thermoelectric energy generation has been used on many unmanned spacecraft. Without any maintenance, they have sometimes continued to provide power well beyond the lengths of the space missions (Wood 1988). Though thermoelectric energy conversion is highly dependable, it does have one

significant weakness: low conversion efficiency.
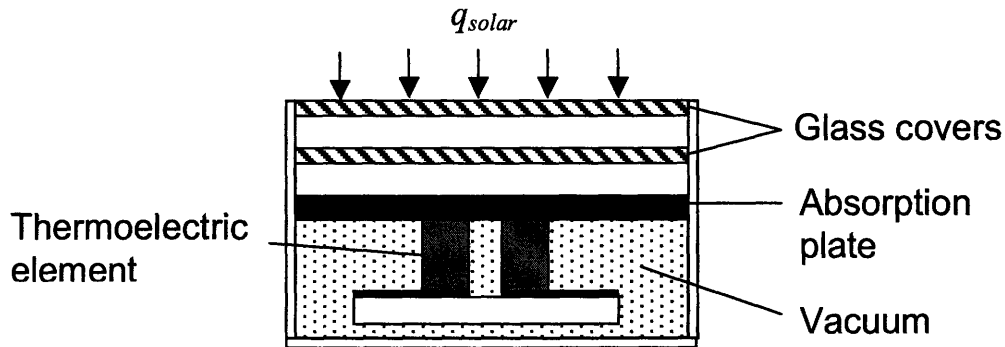
Figure 1.2: A schematic of the specific solar thermoelectric energy generator analyzed.

1.3 Efficiency

The most significant area for improvement for solar thermoelectric energy conversion devices are in their efficiencies. The efficiency of thermoelectric energy conversion η_{TE} is the ratio of useable energy to the heat energy input.

$$\eta_{TE} = \frac{W}{Q_{in}}$$

(1.1)

So far, thermoelectric elements have achieved only very low efficiencies (Telkes 1954). Improvements in their efficiencies can be made primarily through materials selected for use in a thermoelectric element. Comparisons between conductors, insulators, and semiconductors, taking into consideration their crystallization properties and possibilities for doping, address efficiency concerns and are explored in a later section.

The efficiency of the solar energy collector is the focus of this paper. Efficiency in a solar collector is defined as the useable output energy over the total solar radiation incident on the collector.

$$\eta_{SC} = \frac{Q_u}{I_T} \qquad (1.2)$$

Useable energy Q_u is defined as the energy collected, $Q_{s(abs)}$, minus the energy lost

through leakage, Q_{loss}.

$$Q_u = Q_{s(abs)} - Q_{loss} \qquad (1.3)$$

The useable energy output from the solar collector is equivalent to the input

energy of the TE, or $Q_u = Q_{in}$. To increase the efficiency of a solar collector, one must

decrease energy losses through leakage. These values can be changed through materials

selection, geometric parameters, or any number of factors. A thorough thermal analysis

of one particular solar collector shown in figure 1.2, a flat-plate collector with two glass

covers, will explore these two quantities that affect the useable output energy of the solar

collector. In the case of a thermoelectric generator, the output energy of the collector

appears in the form of the temperature of the absorption plate, which is the hot junction

of the TE. With an increase in the temperature of the hot junction, the efficiency of the

whole energy generation system increase.

Chapter 2: Thermoelectric Energy

2.1 Principles

The thermoelectric conversion of thermal energy into electric energy can be understood through the analogy between thermal and electrical elements. Heat transfer textbooks often illustrate concepts of conduction through their electrical analogues, beginning with heat Q and current I. In the case of thermoelectric energy conversion, the analogues become reality as a forced temperature difference ΔT is directly converted into measurable voltage difference ΔV. This phenomenon, called the Seebeck effect, is one of the three underlying principle in thermoelectric energy conversion.

In 1822, Seebeck published his discovery that when opposite ends of a conductor are held at two different temperatures, a current is produced. For materials a and b in series, Seebeck found that the relationship between a small junction temperature differential dT and the generated voltage differential dV were related through a constant $S_{a,b}$, or the Seebeck coefficient.

$$S_{a,b} = -\frac{dV}{dT} \qquad (2.1)$$

The principle is illustrated in Figure 2.1. In this particular illustration, sign convention for the Seebeck coefficient is positive for an induced current flowing from a to b at junction 1. The magnitude of the Seebeck coefficient depends on the temperature of each junction and the material properties of the conductors.
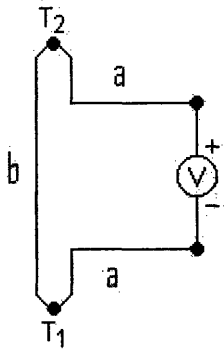
Figure 2.1: The circuit illustrating the Seebeck effect in which a current is generated through the forced temperature difference T_2-T_1.

In a related study, Peltier (1834) found that a small current applied through two conductors in series resulted in heat absorption or generation at their junctions. Peltier defined the relationship between this heat exchange rate Q and the applied current I with equation 2.2, which introduces a constant of proportionality $\pi_{a,b}$ known as the Peltier coefficient.

$$Q = \pi_{a,b} I \qquad (2.2)$$

Positive heat flow, Q, represents heat absorption in the system, and I is positive when current from the colder to the hotter junction. The magnitude and sign of the Peltier coefficient depends on junction temperature and the material properties of each conductor.

By seeking the relationship between Seebeck and Peltier coefficients, Thomson (1854) discovered a third thermoelectric effect. He found that for the same circuit configuration that illustrates the Seebeck and Peltier effects, both a current and a temperature differential through the conductors leads to an additional heat exchange in

each individual conductor. For each conductor, Thomson defined a heat flux per geometric unit given the constant of proportionality τ, or the Thomson coefficient.

$$\frac{dQ}{ds} = \tau \frac{dT}{ds} \tag{2.3}$$

The sign convention for heat exchange and current is identical to the Peltier case.

The Peltier and Thomson coefficients can both be derived from the Seebeck coefficient, which is easily measured in most cases, by equations 2.4 and 2.5.

$$\tau_a - \tau_b = T \frac{dS_{a,b}}{dT} \tag{2.4}$$

$$\pi_{a,b} = S_{a,b} T \tag{2.5}$$

The validity of these two relationships, also derived by Thomson, has been confirmed through experiment (Nolas et al. 2001).

2.2 Efficiency

What is the significance of these three thermoelectric effects? The Peltier effect has already been used in cooling and refrigeration applications. In light of power generation, thermoelectricity can be used to turn natural sources of heat into useable electric energy. The effectiveness and efficiency of energy conversion, however, may limit its applications.
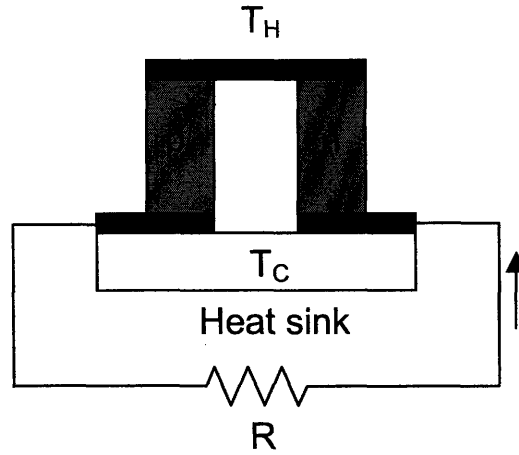
Figure 2.2: The electrical setup of a thermoelectric power generator with p- and n-type elements, hot and cold junctions, and load R.

The conversion efficiency of a thermoelectric energy conversion setup, as shown in figure 2.2, is dependent on several variables, including the temperature at each junction, the Seebeck coefficient at each junction, and the electrical conductivity and thermal resistivity of each conductor. The last three variables are combined into one factor, Z, known as the figure of merit.

$$Z = \frac{(S_1 - S_2)^2}{\left[(\rho_1 \lambda_1)^{\frac{1}{2}} + (\rho_2 \lambda_2)^{\frac{1}{2}} \right]^2}$$

(2.6)

In equation 2.6, ρ is the electrical resistivity and λ is the thermal conductivity. The value of Z for each energy generation setup determines the efficiency of energy conversion. The maximum efficiency of the standard setup for thermoelectric energy conversion, illustrated in figure 2.2, is shown in the following equation.

$$\zeta_{max} = \frac{T_H - T_C}{T_H} \frac{M - 1}{M + \frac{T_C}{T_H}}, \text{ where}$$

(2.7)

$$M = \left[1 + \frac{1}{2}Z(T_H + T_C)\right]^{\frac{1}{2}} \qquad (2.8)$$

The first term stands for the Carnot efficiency, which limits the efficiency of the thermoelectric conversion. The efficiency equation shows that in order to maximize efficiency, the value of Z should have a high value over as large of a temperature range as possible. The value of Z for individual materials can be found by equation 1.9.

$$Z = \frac{S^2}{\rho\lambda} = \frac{S^2\sigma}{\lambda} \qquad (2.9)$$

For convenience, the electrical property is expressed in terms of electrical conductivity σ rather than resistivity. Because the Seebeck coefficient and electrical conductivity can be experimentally determined with relative ease, the ideal material for efficient thermoelectric energy conversion can be selected by optimizing the values of S and σ to achieve a maximized Z value. The figure of merit is commonly used in the dimensionless form ZT, where T is temperature. Materials with the highest ZT values, in addition to other properties such as functionality over a large temperature range, as well as practical access and ease of use, are the best suited to thermoelectric energy conversion. The plot shown in figure 2.3 shows the optimization of both variables.
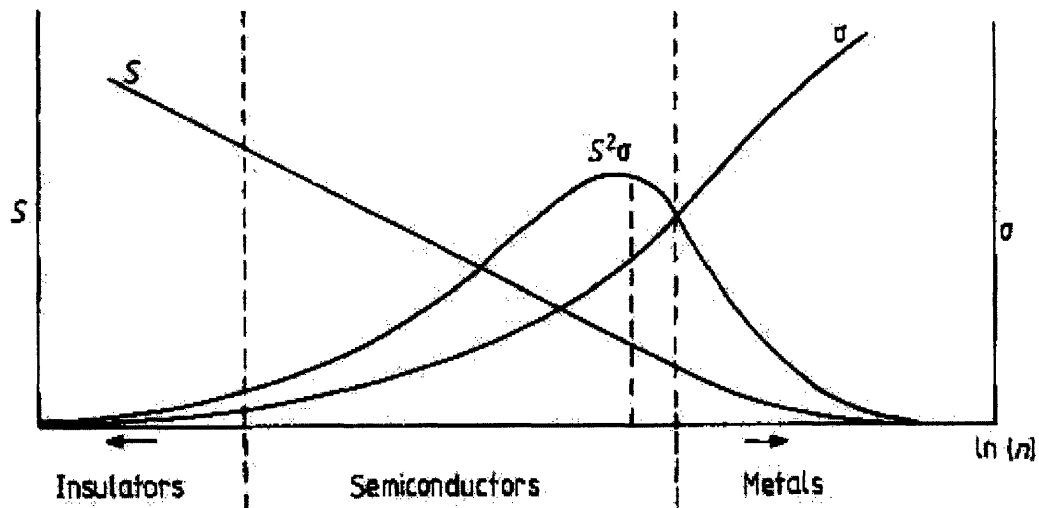
Figure 2.3: Optimized Seebeck coefficient and conductivity of potential thermoelectric materials.[1]

To achieve the highest conversion efficiency in thermoelectric energy generation, the best materials available are semiconductors of $ZT \sim 1$ such as bismuth telluride and alloys of antimony. At this level, thermoelectric generators operate at only 10% of Carnot efficiency. Simply increasing ZT to 4 would lead to an efficiency of 30% of the Carnot efficiency. However, efforts to find materials of higher ZT or to increase the value of ZT beyond 1 in existing materials have barely progressed since the 1950's (DiSalvo 1999).

A solid-state approach to the material in question may allow for the development of a material doped precisely to the characteristics of the ideal semiconductor and achieving the much higher ZT values in a thermoelectric material. Advances continue to be made, but the current unpredictability of new materials structures means that the efforts towards improvement have so far been unsystematic.

---

[1] Figure from C. Wood, "Materials for thermoelectric energy conversion," <u>Reports on Progress in Physics</u>, 51 (1988) 474.

Chapter 3: Solar Energy Collection

The second area of focus on the topic of solar thermoelectric energy conversion efficiency is the conversion of solar energy into thermal energy. Solar energy, though incredibly abundant, is difficult to harness efficiently. The movement of the sun relative to the earth causes continuous variation in levels of sun energy reaching a collector. In addition, the changing of the seasons, as well as day-to-day weather conditions such as cloud cover, limit the amount of useable solar energy. The function of solar collectors is to collect as much solar energy as possible, then to convert it as efficiently as possible into thermal energy without excessive heat loss. There are two major types of solar collectors: flat plate collectors and solar concentrators. Within these types are several variations, including combinations of the two, all aimed at increasing the efficiency of solar energy conversion.

3.1   Flat Plate Collector

One of the most common forms of solar energy collectors, flat plate collectors are typically used as solar air or water heaters but can also be used with thermoelectric converters. As shown in figure 3.1, they essentially consist of a surface that absorbs sunlight and conducts the trapped energy to its target heat exchanger, which either directs the heat to a pipe of flowing fluid or maintains the temperature of the hot junction in a TE. The flat plate collector can include many elements, but their most critical are the absorption plate and clear glazing to ensure that heat does not escape through the surface once absorbed. Their efficiency depends on two major areas: 1) how much heat they are

able to absorb through the surface, and 2) how much heat they are able to contain or transfer with minimal losses.
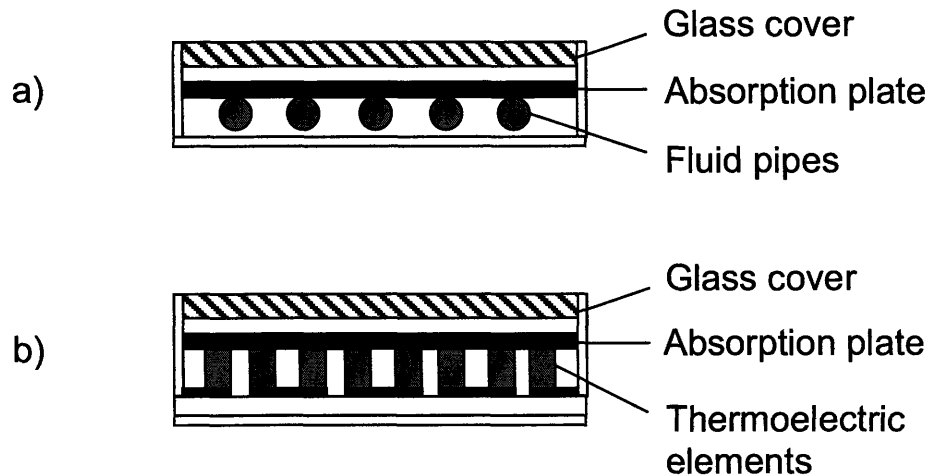

Figure 3.1: Flat plate collector setups for a) an air or water heater, and b) a thermoelectric generator.

3.1.1 Heat Absorption

The form of solar energy absorbed by a flat plate collector is radiation. To achieve the highest energy absorption with the lowest losses, the ideal characteristics of these plates are high absorptance and poor emissivity. Copper, aluminum, and steel are typically used for this purpose because of their high thermal conductivity, which allows for the easy transfer of heat, and high electrical conductivity, which completes the circuit in the thermoelectric component. However, the low absorptance of these metals in the solar spectrum means they require a high-absorptance surface coating to be used as absorption plates. The general term for energy absorbed by a plate per unit area is represented by equation 3.1 (Tiwari 2002).

$$q_{ab} = (\tau\alpha)_{prod} I \qquad (3.1)$$

The transmittance τ of a translucent material is, as shown in figure 3.2, the fraction of radiation that passes completely through. The absorptance α is the amount of radiation that the material absorbs as thermal energy. In equation 3.1, $(\tau\alpha)_{prod}$ is the transmittance-absorptance product. This term is not a direct multiplication of the transmittance and absorptance of the same material. Rather, it is a function of the cover's transmittance and the plate's absorptance, and it determines the amount of energy absorbed by the plate by taking into account the energy transmitted through the cover system.
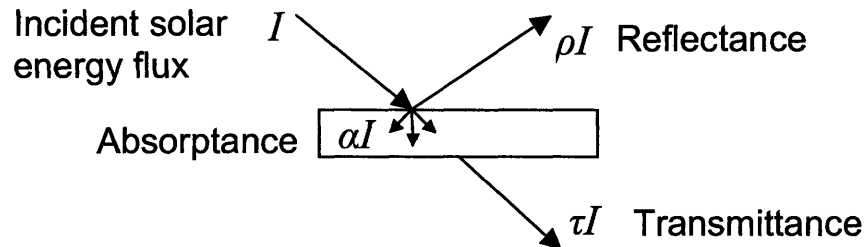
Incident solar energy flux I ρI Reflectance

Absorptance $\boxed{\alpha I}$

τI Transmittance

Figure 3.2: The breakdown of solar energy as it strikes a translucent material.[2]

I in equation 3.1 is the incident solar radiation. Incident solar radiation is the sum of beam and diffuse solar radiation that strikes a surface, and both types can be absorbed by flat plate collector systems. On a sunny day, diffuse radiation can make up as much as 10 to 20% of total solar radiation. On cloudy days, the ratio of diffuse radiation increases up to 100%.

3.1.2 Heat Loss

The rate of heat loss through the top surface of the plate is represented by the following equation.

---

[2] Figure from John H. Lienhard IV and John H. Lienhard V, <u>A Heat Transfer Textbook</u>, (Cambridge, MA: Phlogiston Press, 2006) 29.

$$q_{loss(t)} = A_t U_T \left(T_p - T_a \right) \qquad (3.2)$$

The two temperature variables stand for plate and ambient temperature. The top loss

coefficient is U_T. The efficiency of the plate absorber is represented by the useable

energy retained over the incident solar radiation on the plate.

$$\eta_{plate} = \frac{q_u}{\tau_c I} \qquad (3.3)$$

In the case of the flat plate collector, efficiency depends on four major areas: the

transmittance and absorptance of the selected material, heat loss through the plate

surface, plate and ambient air temperature differences, and incident solar radiation.

Greater efficiency of absorption can be achieved through cover materials of higher

transmittance and plates of higher absorptance. Further, as the temperature difference

between the plate and the ambient air increases, the efficiency of absorption decreases.

These controllable factors must be taken into account in designing a more efficient flat

plate collector for solar energy.

3.2 Solar Concentrator

The principle behind a solar concentrator is that the source of radiation, sunlight,

is focused through the use of an optical device to an increased energy flux on a small

region. Because of the small size of the absorbing plate, heat losses are much less than

for an equivalent flat plate collector at the same temperature. Consequently, any

potential temperature transient effects are also lessened as the system reaches steady state

more quickly. Concentrators can also operate in a much higher temperature range than

flat plate collectors, from 100 to 500°C, which means they have potential for increased

thermoelectric energy generation over flat plate collectors. Additionally, the use of solar

concentrators in TE generators means that there are fewer energy conversion units

required in the entire generator system than there are required in flat plate collector
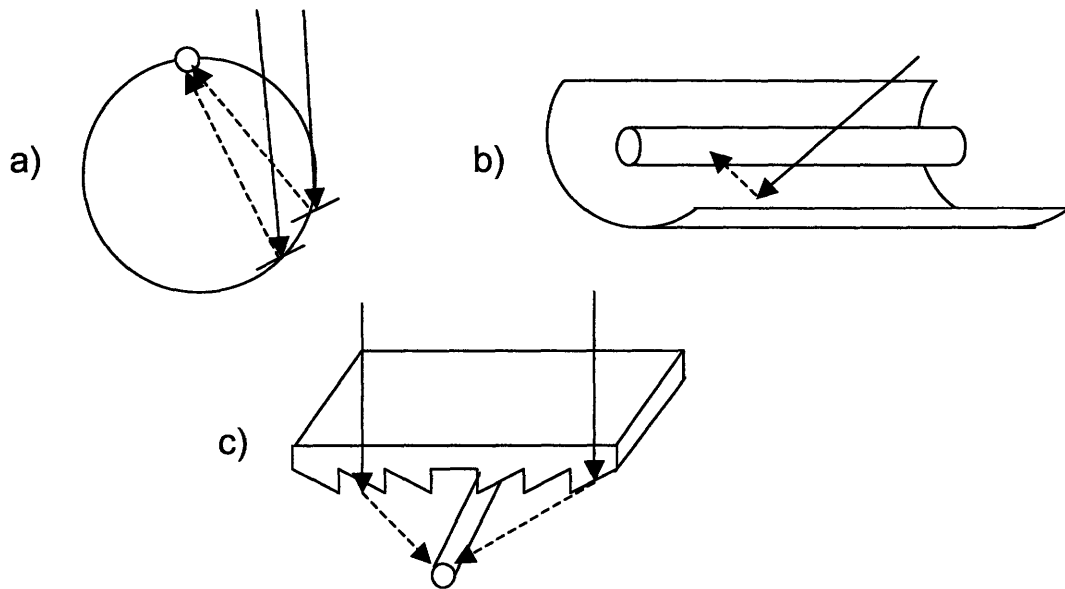
systems.

Figure 3.3: Three possible configurations for tracking solar concentrators: a) the
fixed mirror solar concentrator (FMSC), b) a cylindrical parabolic
concentrator, and c) the linear Fresnel lens concentrator[3].

Problems with solar concentrators include the fact that the small device depends

heavily on beam radiation, so they often must be engineered to follow the movement of

the sun. They also require more maintenance than flat plate collectors because of the

continuous motion of the system, their higher operation temperatures, and their optical

components. Additionally, many solar concentrators cannot collect energy from diffuse

radiation; for the most part they rely solely on beam radiation.

---

[3] Figure from G.N. Tiwari, Solar Energy: Fundamentals, Design, Modeling and Applications, (New York: CRC Press, 2002) 255-256.

Concentrator collectors can be broken into two broad types, tracking and non-tracking, as well as several subcategories: reflecting vs. refracting, line focusing or point focusing, non-imaging vs. imaging. Examples of tracking concentrators include the fixed mirror solar concentrator (FMSC), the cylindrical parabolic concentrator, the linear Fresnel lens concentrator, the paraboloidal dish concentrator, the central tower receiver, the circular Fresnel lens, and the hemispherical bowl mirror. These different tracking concentrators vary between one-axis and two-axis tracking. Figure 3.3 illustrates a few of these concentrators. Examples of the other major type, non-tracking, include everything from a flat receiver with a booster mirror to the popular compound parabolic concentrator (CPC) as shown in figure 3.4. Non-tracking concentrators tend to have a wide aperture and often resemble flat plate receivers with reflecting flat or curved walls.
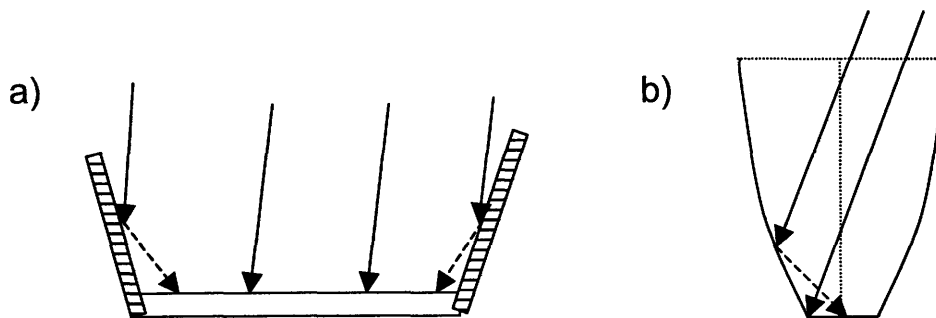
Figure 3.4: Two examples of non-tracking solar concentrators: a) a flat receiver with booster mirror, and b) a compound parabolic concentrator.

Non-imaging concentrators are useful for the purpose of solar energy collection because they are accepting of all radiation, beam and diffuse, over a large range of angles of incidence. As a result, non-imaging concentrators have less sun-tracking requirements than many of their counterparts and as such can be used seasonally. One major type of non-imaging non-tracking solar concentrator, the compound parabolic concentrator (CPC), is commonly used for solar energy collection. The structure of the concentrator is

illustrated in further detail in figure 3.5. As shown, the CPC is characterized by its

acceptance half-angle θ_c, aperture area A_a, and receiver area A_r.
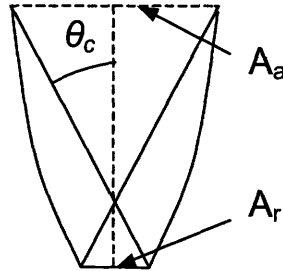
Figure 3.5: Physical parameters of a compound parabolic concentrator (CPC).

A measure of the effectiveness of a concentrator is its concentration ratio, which

is the ratio of the area of the aperture to the area of the receiver. In the case of a linear

concentrator, like the parabola, the concentration radio is found by equation 3.4.

$$\left(\frac{A_a}{A_r}\right)_{linear} = \frac{1}{\sin\theta_c} \tag{3.4}$$

Because the upper sides of a CPC do not significantly contribute to the radiation

reaching the reflector, the parabola is often truncated to save reflector surface area

without reducing radiation. For all these reasons, CPC's are one of the most common

types of solar collector.

Chapter 4: Thermal Analysis of a Flat Plate Collector

4.1 Problem Description

As mentioned in section 3.1, flat plate collectors typically include an absorber plate and glazing. The following analysis looks at a collector with a single flat copper absorption plate with two glass sheets, separated by layers of air, above the plate (figure 4.1). It is assumed that the walls of the collector are near-perfect insulators, so edge effects are ignored. The open region in the lower portion of the converter is a vacuum to reduce convection losses from the TE. Relevant properties of all materials are given in table 4.1.

The analysis of the solar energy collection system begins with the application of the first law of thermodynamics. Ultimately, the analysis will lead to an accurate calculation of the value of useable energy Q_u entering the thermoelectric element.

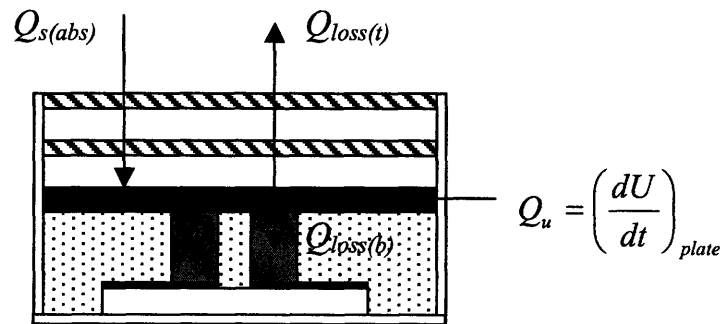$$Q_u = \left(\frac{dU}{dt}\right)_{plate}$$

Figure 4.1: An illustration of the energy exchange in a solar thermoelectric energy converter with a two-glass cover flat plate collector and absorber plate.

The first law applied to the system yields equation 4.1.

$$Q_{S(abs)} = Q_u + Q_{loss} = Q_u + Q_{loss(t)} + Q_{loss(b)} \tag{4.1}$$

By taking into account the area of the two glass insulating covers, the absorption plate, and the thermoelectric elements, the first law equation can be rewritten in terms of heat flux.

$$A_t q_{s(abs)} = Q_u + \left(A_t q_{loss(t)} + A_{TE} q_{loss(b)} \right)$$ (4.2)

Equation 4.2 includes losses $q_{loss(t)}$ through the top of the absorption plate and losses $q_{loss(b)}$ through the thermoelectric elements.
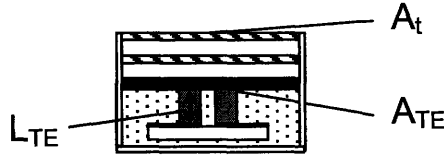

Figure 4.2: Relevant geometries of the system, including the area of the top surfaces and the area and length of the TE.

The analysis of the flat plate collector shown in figure 4.1 is twofold. The first part involves calculating the amount of solar radiation absorbed by the absorption plate. As discussed in section 3.1.1, because of the glass insulating covers, the total incident solar radiation I_T, used to calculate collector efficiency η, is greater than the actual energy $q_{s(abs)}$ absorbed by the plate. The second part of the analysis is to find the values of $q_{loss(t)}$ and $q_{loss(b)}$, or the amount of energy leaked by the absorption plate. By calculating $q_{s(abs)}$ and the two components of q_{loss}, one can find the value of Q_u, or thermal energy to the thermoelectric element.

$$Q_u = A_t q_{s(abs)} - A_t q_{loss(t)} - A_{TE} q_{loss(b)}$$ (4.3)

Once Q_u is known, the efficiency of the collector system can be found using equation 1.2.

$$\eta_{SC} = \frac{Q_u}{I_T} \qquad\qquad (1.2)$$

4.2 Calculation of Absorbed Solar Energy

Solar radiation entering the collector is represented by I_T, which stands for the total incident solar energy. As shown earlier in figure 3.2, energy passing through a translucent surface is split into transmitted (τ), reflected (ρ), or absorbed (α) energy. The ratios of the division depend on surface and material characteristics. In the case of the flat plate collector, glass is used as a cover for its typically high transmittance τ, low absorptance α, and low reflectance ρ. This choice of material minimizes energy lost through the insulating covers. Similarly, the absorbing plate should have high absorptance and low transmittance and reflectance to maximize the energy absorbed by the plate.

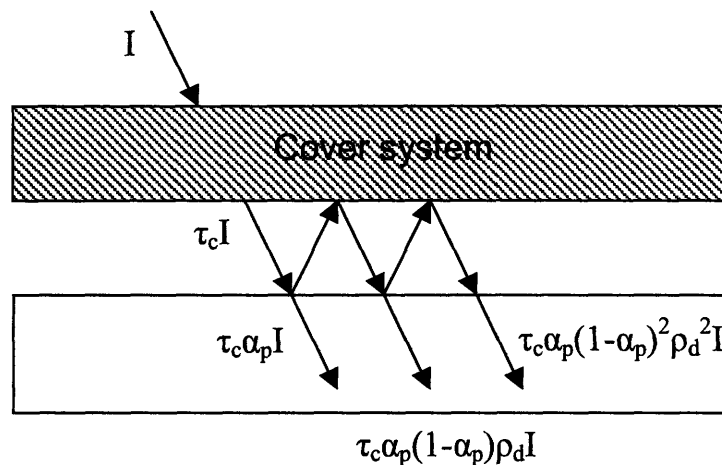**Figure 4.3**: The breakdown of incident radiation, as affected by the transmittance of the cover system τ_c, the absorptance of the plate α_p, and the reflectance of the bottom surface of the cover system ρ_d.[4]

[4] Figure from John A. Duffie and Willian A. Beckman, Solar Engineering of Thermal Processes, (Hoboken, New Jersey: John Wiley & Sons, Inc., 2006) 215.

In the case of a collector system with multiple covers, energy transmitted to the plate is partially absorbed, partially reflected back to the covers, partially reflected back to the plate, where it is again partially absorbed and reflected. In this way, not all energy reflected from the plate is lost. To measure the fraction of energy actually absorbed by a plate under a cover system, the transmittance-absorptance produce $(\tau\alpha)_{prod}$ was developed. As shown in section 3.1.1, the incident energy absorbed by a surface under a cover system is represented by $(\tau\alpha)_{prod}I$. The product is not literally a product; rather, the value of $(\tau\alpha)_{prod}$ is represented by equation 4.4.

$$\left(\tau\alpha\right)_{prod} = \frac{\tau_c\alpha_p}{1-(1-\alpha_p)\rho_d} \tag{4.4}$$

Equation 4.5, an empirical relation, applies to collectors with up to two covers made of ordinary glass (Duffie 2006). To find the value of the product, one must independently calculate the transmittance of the cover system and find the absorptance of the plate.

$$\left(\tau\alpha\right)_{prod} \cong 1.02\tau_c\alpha_p \tag{4.5}$$

The transmittance for the cover system is dependant on several characteristics of the covers. Because energy transmission dominates in the case of glass covers, the total transmittance is calculated by considering absorption and reflection losses. It has been found empirically that the total transmittance τ can be approximated as the product of transmittance accounting for absorption losses, τ_a, and transmittance accounting for reflection losses, τ_r.

$$\tau \cong \tau_a\tau_r \tag{4.6}$$

$$\tau_a = \exp\left(-\frac{KL}{\cos\theta_2}\right) \qquad\qquad (4.7)$$

Absorption losses take into account the extinction coefficient K of glass as well as its

thickness L.

$$\tau_r = \frac{1}{2}\left(\frac{1-r_\parallel}{1+3r_\parallel} + \frac{1-r_\perp}{1+3r_\perp}\right), \text{ where} \qquad\qquad (4.8)$$

$$r_\perp = \frac{\sin^2(\theta_2-\theta_1)}{\sin^2(\theta_2+\theta_1)}$$

$$r_\parallel = \frac{\tan^2(\theta_2-\theta_1)}{\tan^2(\theta_2+\theta_1)}$$

Transmittance with reflection losses is determined through angles of incidence of the

radiation. The angles θ_1 and θ_2 are the angles of incidence of the sunlight as it travels

through air, strikes the glass, and is refracted by the glass. Figure 4.4 illustrates this
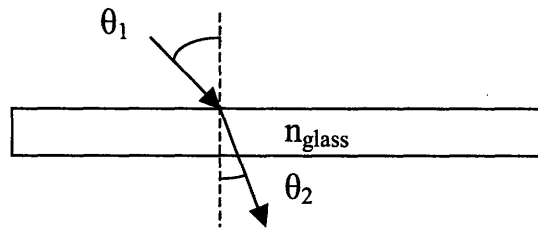
effect.

Figure 4.4: An illustration of Snell's law as it applies to a glass cover.

Because air has a refraction index of $n = 1$, Snell's law determines the refraction

angle through a glass cover as a function of angle of incidence and n_{glass}, which typically

has a value of 1.526 (Duffie 2006).

$$\theta_2 = \sin^{-1}\left(\frac{\sin\theta_1}{n_{glass}}\right) \tag{4.9}$$

Since absorption dominates as radiation strikes the plate, the value of α in the transmittance-absorptance product is the value for the specific surface of the plate. Absorption plates are often painted black for their large value of α.

In the case of the two-glass flat plate collector, the transmittance-absorptance product cannot be applied to the total solar radiation as generalized in equation 3.1 because there are several different spatial distributions of solar radiation. Solar energy entering the collector can be broken into three types: beam, diffuse, and ground. The distinct incident radiation of each type means that each has a unique transmittance value and a unique transmittance-absorptance product. Beam radiation is the direct solar radiation that has not been scattered by the atmosphere. Diffuse radiation, sometimes called sky radiation, is the solar energy that has been redirected by the atmosphere. Ground-reflected radiation occurs as solar energy reflected off the ground is directed into the collector; this effect is only applicable in the case of collectors tilted at an angle to the horizontal β.

Total solar radiation consists of the sum of beam and diffuse radiation.

$$I_T = I_b + I_d \tag{4.10}$$

To determine the individual values for beam and diffuse radiation, one must apply the ratio I_d/I, which is a function of k_T or hourly clearness index. This variable is defined as the ratio of total solar radiation on a horizontal surface to hourly extraterrestrial radiation.

$$k_T = \frac{I}{I_0} \qquad (4.11)$$

Values for I_0 can be calculated with accuracy given the solar constant, day of the year, latitude, and other such parameters. For the purpose of this analysis, the value of I_o is found from recorded data.

Once k_T is known, the value of diffuse radiation can be determined using the following correlation developed by Orgill and Hollands (1977).

$$\frac{I_d}{I} = \begin{cases} 1.0 - 0.249 k_T & \text{for } k_T \leq 0.22 \\ 1.557 - 1.84 k_T & \text{for } 0.22 < k_T \leq 0.8 \\ 0.177 & \text{for } k_T > 0.8 \end{cases} \qquad (4.12)$$

To determine the solar energy absorbed by the absorbing plate, one must account for beam, diffuse, and ground radiation individually because of their unique angles of incidence. Equation 4.13 shows the total absorbed solar radiation, S, for a cover-plate collector system.

$$S = I_b R_b (\tau\alpha)_{prod(b)} + I_d (\tau\alpha)_{prod(d)} \left(\frac{1 + \cos\beta}{2} \right) + \rho_g I(\tau\alpha)_{prod(g)} \left(\frac{1 - \cos\beta}{2} \right) \qquad (4.13)$$

The transmittance for ground and diffuse radiation are determined through an effective angle of incidence as a function of collector tilt β. As mentioned previously, the absorptance in all cases is the value of α_c for the plate and is therefore constant between all three radiation types.

Absorbed solar energy S is equal to the value $q_{s(abs)}$ in equation 4.3. Once $q_{s(abs)}$ is known, only the calculation of q_{loss} is left to determine the value of useable energy Q_u.

4.3 Calculation of Energy Lost from Absorption Plate

Once energy $q_{s(abs)}$ is absorbed by the plate, the plate would ideally retain all energy and achieve as high a temperature as possible for maximum energy generation through the thermoelectric effect. Unfortunately, the plate cannot retain all the heat it absorbs. Losses occur through convection and radiation from the top of the plate and through conduction from the bottom. Figure 4.5 shows in full detail the heat losses for each cover and plate.
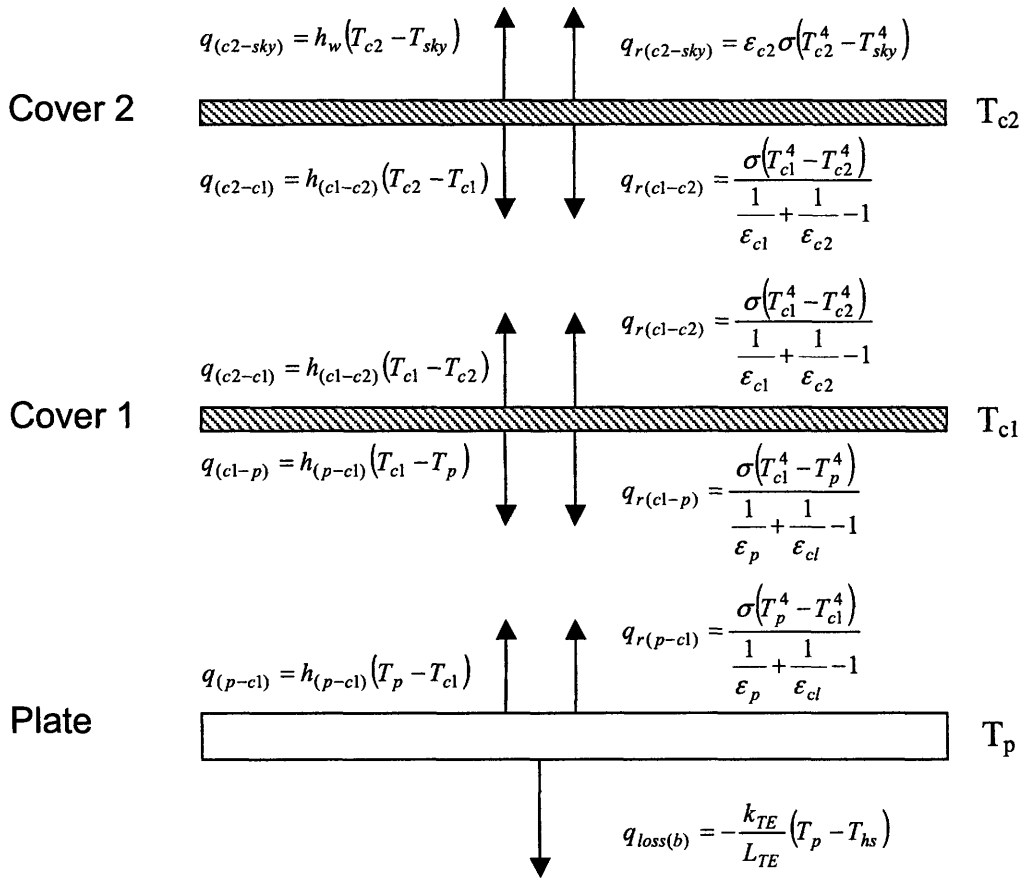

Figure 4.5: A detailed diagram of heat losses for each glass cover and the absorption plate.

The first law equation for the absorption plate is equation 4.1.

$$A_t q_s - A_t q_{l(t)} - A_{TE} q_{l(b)} = mc \frac{dT_p}{dt} \qquad (4.14)$$

This equation can be solved for the maximum temperature achieved by the plate, which occurs when the system reaches steady-state or when the term dT_p/dt goes to zero. Top losses are represented by equations 4.15 and bottom losses by equation 4.16.

$$q_{l(t)} = U_T (T_p - T_a) \qquad (4.15)$$

$$q_{l(b)} = -\frac{k_{TE}}{L_{TE}} (T_p - T_{hs}) \qquad (4.16)$$

When substituted into the steady-state version of equation 4.14 and solved for T_p, equation 4.17 results.

$$T_p = \frac{A_t U_T T_a - A_{TE} \dfrac{k_{TE}}{L_{TE}} T_{hs}}{A_t U_T - A_{TE} \dfrac{k_{TE}}{L_{TE}}} \qquad (4.17)$$

All constants are known except for the overall heat transfer coefficient U_T. Energy lost from the top of the plate to the surroundings is dependent on the top loss coefficient, which can be determined through the concept of combined thermal resistance. Figure 4.6 illustrates the thermal circuit from the plate to the air above the top glass cover. Glass covers 1, 2, and the absorption plate are assumed to have uniform temperatures. Thermal resistance occurs in the form of convection and radiation resistance between the plate and cover 1, cover 1 and cover 2, and cover 2 and the sky.
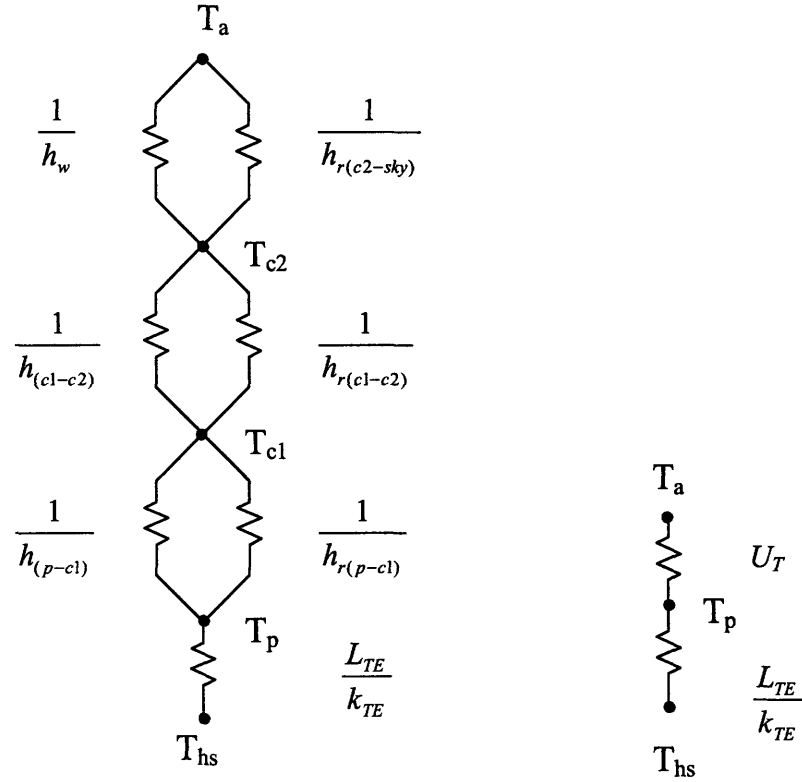
Figure 4.6: The a) thermal circuit of the collector system and b) equivalent circuit with combined top loss coefficient U_T.

The energy loss through the top of the plate is defined by the sum of energy lost by convection and by radiation, where σ is the Stefan-Bolztman constant and ε_p and ε_{cl} represent the emittance of the plate and cover 1.

$$q_{l(p-cl)} = h_{p-cl}(T_p - T_{cl}) - \frac{\sigma(T_p^4 - T_{cl}^4)}{\dfrac{1}{\varepsilon_p} + \dfrac{1}{\varepsilon_{cl}} - 1} \qquad (4.18)$$

It is convenient to use the definition of radiation heat transfer coefficient to define a single resistance R_l for the heat transfer from the absorption plate to cover 1.

$$q_{l(p-cl)} = (h_{(p-cl)} + h_{r(p-cl)})(T_p - T_{cl}), \text{ where} \qquad (4.19)$$

34

$$h_{r(p-cl)} = \frac{\sigma(T_p + T_{cl})(T_p{}^2 + T_{cl}{}^2)}{\dfrac{1}{\varepsilon_p} + \dfrac{1}{\varepsilon_{cl}} - 1}$$ (4.20)

A similar procedure is applied to heat transfer coefficients for all three areas of resistance.

$$R_1 = \frac{1}{h_{(p-cl)} + h_{r(p-cl)}}$$ (4.21)

$$R_2 = \frac{1}{h_{(cl-c2)} + h_{r(cl-c2)}}$$ (4.22)

$$R_3 = \frac{1}{h_w + h_{r(c2-sky)}}$$ (4.23)

In each case, the first heat transfer term represents convection and the second represents radiation. When totaled, they result in the overall top loss coefficient.

$$U_T = \frac{1}{R_1 + R_2 + R_3}$$ (4.24)

The problem associated with calculating the top loss coefficient is that each heat individual heat transfer coefficient is dependent on the unknown temperatures of the covers and plate. The approach to solving for the top loss coefficient involves an estimation of maximum and minimum temperatures for each cover or plate. The maximum temperatures of cover 1 and cover 2 were determined by assuming only top losses and no bottom losses for each cover. An iterative process was then used to derive an equation for the time-dependent temperature. However, these equations are a function of the convection heat transfer coefficient, whose calculation also requires plate and

cover temperatures. The temperatures used to determine the convection coefficients were approximated based on ambient air temperature.

There are two unique procedures for finding the convection and radiation heat transfer coefficients.

4.3.1 Convection heat transfer coefficient

The setup of the flat plate collector includes two unique configurations for convection: wind convection off a flat plate, and natural convection between two flat plates. Wind convection can be approximated using the equation formulated by Mitchell (1976) for forced convection over buildings (Duffie 2006).

$$h_w = \frac{8.6 V^{0.6}}{L^{0.4}} \tag{4.25}$$

In this equation, V stands for wind velocity, which has a world average of about 5 m/s. The characteristic length L stands for the cube root of the building volume, in meters. Though the process for determining a wind heat transfer coefficient is not yet refined, Mitchell's equation serves the purpose.

The heat transfer coefficient for natural convection between two flat plates is found using the Hollands et al. (1976) correlation of the Nusselt number for plates at a tilt angle β.

$$Nu = 1 + 1.44 \left[1 - \frac{1708(\sin 1.8\beta)^{1.6}}{Ra\cos\beta} \right] \left[1 - \frac{1708}{Ra\cos\beta} \right]^+ + \left[\left(\frac{Ra\cos\beta}{5830} \right)^{\frac{1}{3}} - 1 \right]^+ \tag{4.26}$$

The superscript plus signs indicate that only positive terms within the brackets should be used. The Raleigh number, Ra, is defined by equation 4.27.

$$Ra = \frac{g\beta\Delta T L^3}{v\alpha}$$ (4.27)

In this equation, L stands for the distance between the plates, g is the gravitational constant, v is the kinematic viscosity of the fluid, and α is its thermal diffusivity. The temperature difference, as mentioned earlier, is approximated based on the ambient air temperature. Once the Nusselt number is known, the heat transfer coefficient can be calculated.

$$h = \frac{k}{L} Nu$$ (4.28)

The variable k stands for the thermal conductivity of the fluid, which is in this case air. This procedure applies to the calculation of $h_{c\text{-}p1}$ and $h_{c1\text{-}c2}$. These values are necessary for the calculation of the radiation heat transfer coefficient.

4.3.2 Radiation heat transfer coefficient

The radiation heat transfer coefficient is defined by a rearrangement of the equation for radiation energy.

$$h_r = \frac{\sigma(T_1 + T_2)(T_1^2 + T_2^2)}{\dfrac{1}{\varepsilon_1} + \dfrac{1}{\varepsilon_2} - 1}$$ (4.29)

To find the closest value of the actual temperatures of the covers and plate to use in the equation for h_r, the minimum and maximum temperatures of each plate were found through an iterative calculation process. In the case of radiation heat transfer between cover 2 and the sky, the steady-state first law without losses to cover 1 was derived.

$$A_t \alpha_{c2} I - A_t h_w (T_{c2} - T_a) - A_t h_{r(c2-sky)} (T_{c2} - T_{sky}) = 0$$ (4.30)

In this equation, α_{c2} is the absorptance of cover 2 and I is the incident solar radiation on the cover. In effect, the product of these two variables is the amount of solar energy absorbed by cover 1. The expression for $h_{r(c2-sky)}$, as a function of T_{c2}, is in the form found in equation 4.29. Solving equation 4.30 for T_{c2} leads to its steady-state value, equation 4.31.

$$T_{c2} = \frac{A_t \alpha_{c2} I + h_w T_a + h_{r(c2-sky)} T_{sky}}{h_w + h_{r(c2-sky)}} \tag{4.31}$$

Because $h_{r(c2-sky)}$ is a function of T_{c2}, the equation is iterated until a value of T_{c2} is found. Then $h_{r(c2-sky-max)}$ is calculated. To find $h_{r(c2-sky-min)}$, the ambient air temperature T_a is substituted for T_{c2}. The final value of $h_{r(c2-sky)}$ used in the analysis is then the average of the minimum and maximum values found. Calculations show that the minimum and maximum heat transfer coefficients vary from each other only by up to 2%, so the value of $h_{r(c2-sky)}$ does not vary significantly over the full range of possible temperatures for each plate. The same method was used to find $h_{r(c1-c2)}$ and $h_{r(p-c1)}$, with similar results.

Once the heat transfer coefficients are calculated, the value of the overall top loss coefficient U_T can be entered into equation 4.17. Entering all values and solving the equation leads to the maximum value of the plate temperature that can be achieved given the absorption and loss properties of the collector. This is also the best achievable value of the hot junction of the thermoelectric element.

$$T_p = \frac{A_t S + A_t U_T T_a - A_{TE} \dfrac{K_{TE}}{L_{TE}} T_{hs}}{A_t U_T - A_{TE} \dfrac{K_{TE}}{L_{TE}}} \tag{4.17}$$

To check the validity of the procedure for determining U_T, the transient equation was solved to determine the time constant of the system. The solution to the transient equation is equation 4.32.

$$T_p(t) = \left(T_a - \frac{A_t U_T T_a - A_{TE} \frac{K_{TE}}{L_{TE}} T_{hs}}{A_t U_T - A_{TE} \frac{K_{TE}}{L_{TE}}} \right) \exp\left(-\frac{A_t U_T - A_{TE} \frac{K_{TE}}{L_{TE}}}{m_p c_p} t \right) + \left(\frac{A_t U_T T_a - A_{TE} \frac{K_{TE}}{L_{TE}} T_{hs}}{A_t U_T - A_{TE} \frac{K_{TE}}{L_{TE}}} \right)$$

The value of Q_u and η_{SC} can now be calculated using equations 4.3 and 1.2.

$$Q_u = A_t q_{s(abs)} - A_t q_{loss(t)} - A_{TE} q_{loss(b)} \qquad (4.3)$$

$$\eta_{SC} = \frac{Q_u}{I_T} \qquad (1.2)$$

To determine the efficiency of the TE given the power output of the thermoelectric element and the input of thermal energy from the solar collector, equation 1.1 is used. The power W is determined by a form of the Seebeck relation.

$$V = IR = (S_p - S_n)(T_H - T_C) \qquad (4.18)$$

$$I = \frac{(S_p - S_n)(T_H - T_C)}{R} \qquad (4.19)$$

$$W = I^2 R = \frac{(S_p - S_n)^2 (T_H - T_C)^2}{R} \qquad (4.20)$$

The resistance can be found with equation 4.21, which includes the resistivity ρ of the TE conductor, the area of the TE A_{TE}, and the length of the TE L_{TE}.

$$R = \frac{L_{TE}\rho}{A_{TE}}$$ (4.21)

A good measure of the effectiveness of the solar thermoelectric generator system is the power output W per unit area of the collector, A_t. A larger collector area will be able to trap a larger amount of solar energy but may also lead to the wastage of space. Ideally, the ratio of the area of the collector A_t to the area of the TE A_{TE} will be as small as possible for the largest possible value of power per unit area of the collector.

4.4 Calculation Results

To determine the characteristics of the flat plate system that most significantly affect the efficiency of the collector, the efficiency was calculated using MATLAB and plotted over several physical parameters of the collector and the thermoelectric element. Constants and assumed values for variables can be found in table 4.1.

Table 4.1: Constants and assumed values used in the analysis.

Glass	
Absorptance	0.04
Emittance	0.94
Transmittance (One sheet)	0.84
Refractive index	1.526
Extinction coefficient (1/m)	4
Absorption plate coating	
Emittance	0.9
Bismuth telluride	
Thermal conductivity (W/mK)	1.2
Temperature (K)	
Sky	291
Air	298
Heat sink	288

Hourly solar radiation (J)	
Incident	1.43x10^6
Extraterrestrial	2.18x10^6

The heat energy rate over increasing collector areas is shown in figure 4.6.

Absorbed solar energy continues to increase linearly with increasing collector area at a

higher rate than leaked heat, so that the system becomes increasingly better at containing

heat. The value of T_p, the temperature of the absorption plate, ranges from 301.7 K to

328.2 K over a collector area range of 0.1 m^2 to 2 m^2. Given a heat sink temperature T_{HS}

= 288 K, the maximum temperature difference driving the power generation is ΔT = 40.2
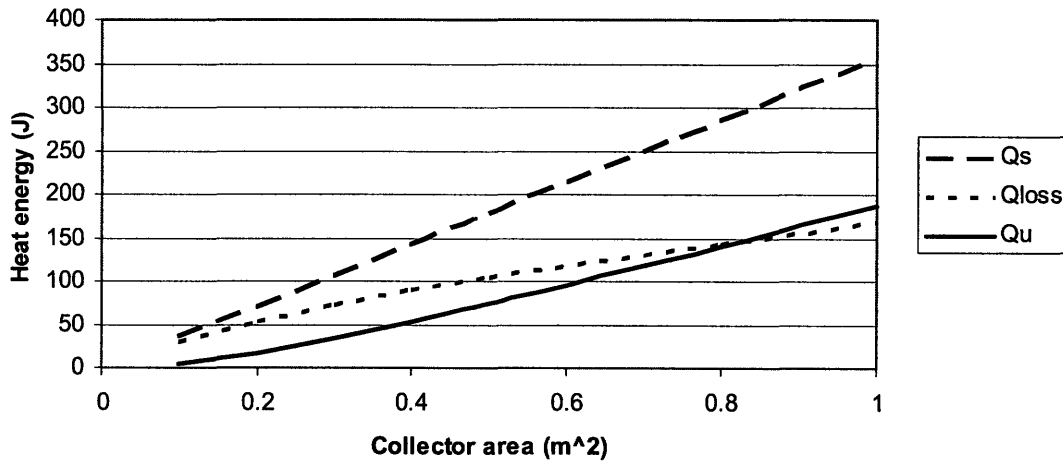
K.

Figure 4.6: The ratios of the thermal energies of the system, where Q_s is solar energy absorbed, Q_{loss} is energy leaked to the environment, and Q_u is energy used to heat the absorption plate to T_p.

Figure 4.7 shows the efficiency of the collector as a function of collector area A_t.

As the area of the collector continues to increase, the absorbed incident radiation $Q_{s(abs)}$

outweighs top losses $Q_{loss(t)}$ until they reach equilibrium. Efficiency follows a negative exponential curve with increasing collector area. The collector efficiency is plotted for three different values of the space between the collector plates, L_{space}. The values for L_{space} are 0.0025 m, 0.025 m, and 0.25 m. As the space between the plates decreases, the collector efficiency increases. The relation likely breaks down as the distance between plates goes to zero because conduction heat transfer to the air between the plates will overtake convection.
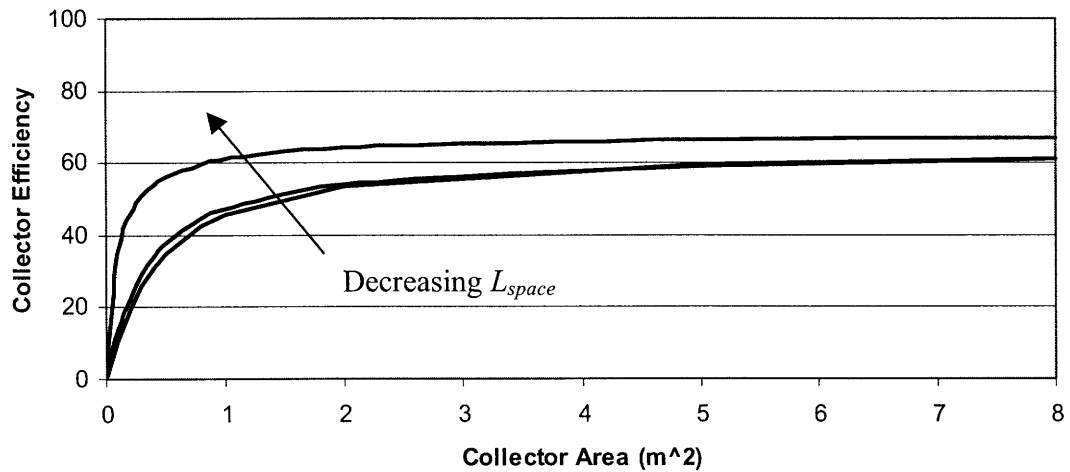

Figure 4.7: A plot of collector efficiency with t_{cover} = 0.003 m as a function of collector area against decreasing space between the plates, L_{space}.

Figure 4.8 shows efficiency as a function of collector area, with varying glass cover thickness t_{cover} for the values 0.001 m, 0.003 m, and 0.01 m. Collector efficiency does not significantly vary as a function of cover thickness within a reasonable range of values.
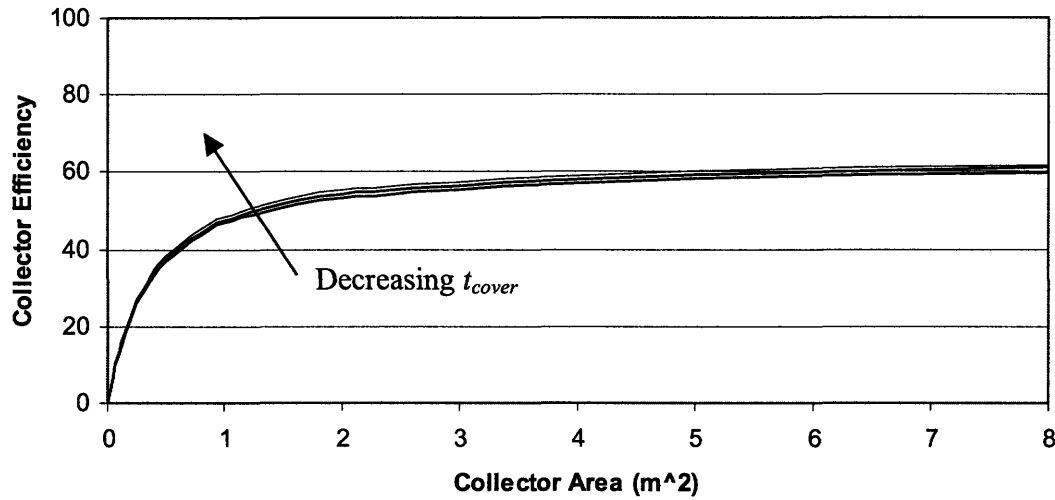
Figure 4.8: A plot of collector efficiency with L_{space} = 0.025 m, as a function of collector area against decreasing glass cover thickness, t_{cover}.

The parameters A_{TE} and L_{TE} of the thermoelectric element also significantly affect the efficiency of the collector system because of losses due to conduction. Though these parameters are not a physical part of the solar collector, their size significantly affects collector efficiency. As A_{TE} goes to zero and L_{TE} increases, the efficiency of the collector increases as well because of the increased thermal resistance of conduction.

Equation 1.1 showed that the efficiency of the thermoelectric element is the output power of the generator over the heat energy absorbed by the hot junction. Figure 4.9 plots the power output of the TE as a function of solar collector area. The parameters held constant in the plot are A_{TE} = 0.001 m^2, L_{TE} = 0.01 m. The thermoelectric material is bismuth telluride, which has a resistivity ρ of 4×10^{-5} Ω^{-1} and Seebeck coefficients of S_p = 81 μV/K and S_n = -288 μV/K. The power output increases at a high rate with increasing collector area until W = 2.5 W, when the area reaches about 0.5 m^2 and the power output begins to taper.
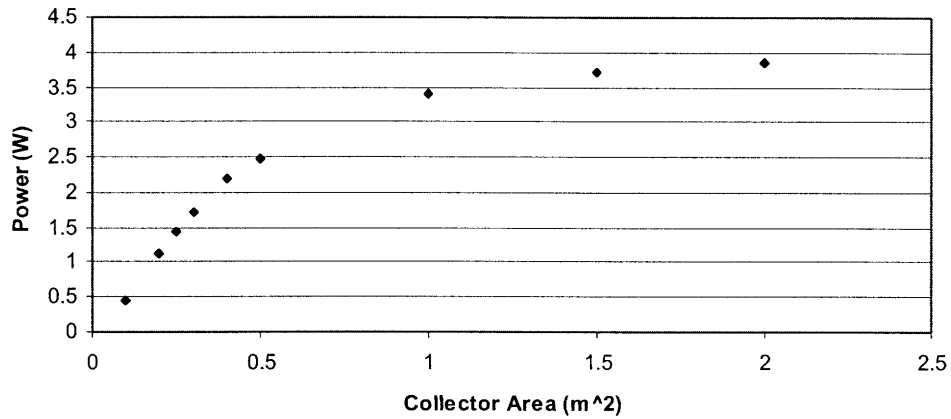
Figure 4.9: The power output of the TE as a function of solar collector area.

The amount of power per unit area of the collector is plotted in figure 4.10. As a function of the ratio between collector area and TE area, A_t/A_{TE}, the power per unit area P/A_t achieves a clear maximum of 5.76 W/m^2 at $A_t/A_{TE} = 250$, where $A_t = 0.25$ m^2 and A_{TE} = 0.001 m^2.
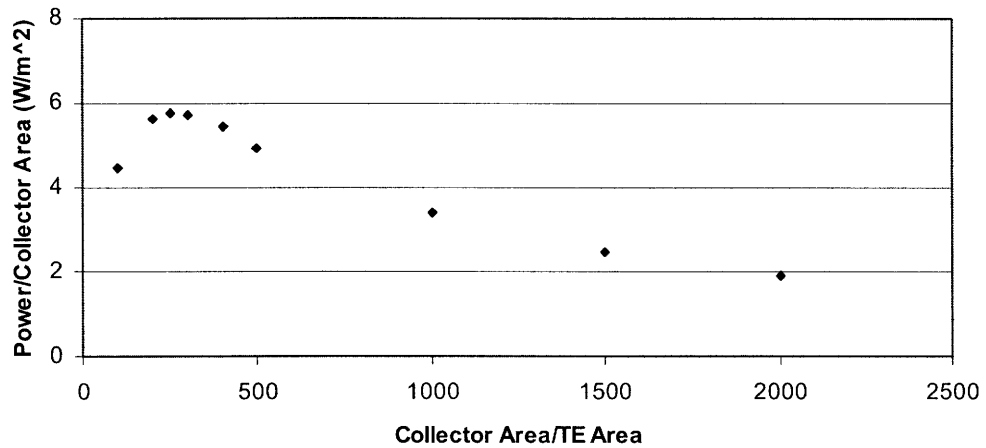

Figure 4.10: A plot showing the power per unit area of the collector as a function of area ratios.

Chapter 5: Summary and Conclusion

Solar thermoelectric energy generation is a significant area of research because of its great potential for the effective and easy harnessing of solar energy. Compared to other forms of solar energy conversion, thermoelectric energy generation is simple, low-maintenance, and dependable. Improvements on its greatest weakness, low efficiency, have been the focus of much research as scientists explore methods of increasing the figure of merit, ZT, in known semiconductors.

Along with improvements in thermoelectrics, the design optimization of efficient solar collectors is an area of continuous study. The two major types of solar collectors, flat-plate and solar concentrators, both have strengths and weaknesses in their abilities to capture and contain thermal energy from solar radiation. Solar concentrators are particularly useful for their ability to maintain high-temperature hot junctions in thermoelectric elements, which increases output power. However, the necessary complexity of solar collectors as a result of their required tracking of the sun makes them less useful on a larger scale. Without need for moving mechanical parts or other complex features, flat-plate collectors are ideal for common, low-cost use. The more efficiently they can capture and contain solar radiation, the greater the power output of the thermoelectric generator.

Areas for improvement in the efficiency of the flat plate collector were determined by the performance of a heat transfer analysis over a two-cover flat plate collector connected to a TE. With the goal of maximizing the absorption plate temperature, which also functioned as the hot junction of the TE, two areas were

analyzed: the flux of solar energy absorbed by the plate, and the flux of energy lost to the environment from the plate. The efficiency of the collector, or the ratio of useable energy output to the incident solar radiation input, was determined for several varied physical parameters including cover spacing, cover thickness, and collector area. Optimization within a reasonable range of physical parameters leads to efficiencies up to 50%. Power output per unit area of the collector was then determined as a function of the ratio of the solar collector area to the area of each thermoelectric element. The power-area ratio maximized at 5.76 W/m^2, at an area-area ratio of 250. Improvements on the design of a flat-plate solar collector should focus on two areas: 1) reducing convection and radiation losses from the hot junction of the thermoelectric element, and 2) decreasing the collector area to TE area ratio for maximum power output per unit area of the collector.

References

DiSalvo, Francis J. "Thermoelectric Cooling and Power Generation." Science 285 (30

    July 1999): 703-706.

Duffie, John A. and William A. Beckman. Solar Engineering of Thermal Processes.

    Hoboken, New Jersey: John Wiley & Sons, Inc., 2006.

Lienhard IV, John H. and John H. Lienhard V. A Heat Transfer Textbook. Cambridge,

    MA: Phlogiston Press, 2006.

Nolas, G.S. et al. Thermoelectrics: Basic Principles and New Materials Developments.

    New York: Springer, 2001.

Orgill, J. F. and K. G. T. Hollands. "Correlation Equation for Hourly Diffuse Radiation

    on a Horizontal Surface." Solar Energy 357 (1977): 19.

Telkes, Maria. "Solar Thermoelectric Generators." Journal of Applied Physics 23:6 (June

    1954): 765-777.

Tiwari, G.N. Solar Energy: Fundamentals, Design, Modeling and Applications. New

    York: CRC Press, 2002.

Wood, C. "Materials for thermoelectric energy conversion." Reports on Progress in

    Physics 51 (1988) 459-539.

Works Consulted

Lenoir, B., et al. "Electrical performance of skutterudites solar thermoelectric

generators." Applied Thermal Engineering 23 (2003): 1407-1415.

Omer, S.A., and D.G. Infield. "Design optimization of thermoelectric devices for solar

power generation." Solar Energy Materials and Solar Cells 53 (1998): 67-82.

Maneewan, S., et al. "Heat gain reduction by means of thermoelectric roof solar

collector." Solar Energy 78 (2005): 495-503.

Min, Gao and Rowe D.M. "Recent Concepts in Thermoelectric Power Generation." 21st

International Conference on Thermoelectronics (2003)

Rowe, D.M., and Gao Min. "Evaluation of thermoelectric modules for power

generation." Journal of Power Sources 73 (1998): 193-198.